DEVELOPMENT AND VALIDATION OF A 3D TIME DEPENDENT MODEL USED FOR THE SIMULATION OF INTERNAL CHARGING AT SPACECRAFT LEVEL

Pierre Sarrailh(1), Thierry Paulmier(1), Bernard Dirassen(1), David Rodgers(2), Giovani Santin(2), Fabrice Cipriani(2), Denis Payan(3)

(1)ONERA, The French Aerospace Lab, 2 Av Edouard Belin, 31055 Toulouse, France, Email: Pierre.Sarrailh@onera.fr
(2)ESA/ESTEC, 2200 AG Noordwijk, The Netherlands, Email: David.Rodgers@esa.int
(3)CNES, Toulouse, France, Email: Denis.Payan@cnes.fr

ABSTRACT

A new model of dielectric conductivities has been implemented in SPIS-IC. It allows modelling the time dependent behaviour of the charge and potential inside payload components. The simulation results have been compared to experiments on four validation cases going from simple 1D geometry to more complex 3D components such as a D-Type connector. The comparison shows a good agreement on most of the cases and the discrepancies are explained in certain cases. Finally, the results have been analysed in term of discharge probability and severity. This study also shows the great importance of time dependant modelling of the radiation induced conductivity.

1. INTRODUCTION

Despite technological progress, the effects of the space radiation environment on spacecraft and their payloads remain a significant source of space mission anomalies. High energy electrons penetrate and interact with internal sub systems. On long time scales, the charge deposit accumulates inside thick dielectrics and can create IESD (internal electrostatic discharges). This internal charging phenomenon, potentially leading to part or system failure, is well known to spacecraft designers and requires efficient shielding to protect vulnerable components of the payload [1]–[4].

In order to assist the designer during the shielding design, ESA has initiated the development of radiation analysis software in the frame of the ELSHIELD project (Energetic Electron Shielding, Charging and Radiation Effects and Margins). This software is based on the GEANT4 [5], [6] library for high energy electron transport in the spacecraft and on SPIS [7], [8] for the deposited charge transport in the payload components. Each part of the software has been validated separately, radiation on one side and charging on the other side. The aim of this paper is to present an extension of the conductivity model previously used and an experimental validation of the overall modelling chain from radiation to charging.

During the course of this study, a specific attention has been paid to the time dependant phenomena and to the 3D aspects of the internal charging problems. In section 2, the internal charging model and the improvements concerning time dependant aspects and conductivity model are described. In the section 3, the experimental setup used to obtain internal charging data is shown. In section 4, the validation protocol is detailed. In section 5, the experimental and numerical results are presented and analysed in two selected cases.

2. INTERNAL CHARGING MODEL

Among others radiation tools, Geant4 has the capabilities to compute local three-dimensional maps of total ionizing dose and deposit charge. Whereas the common use of Geant4 is to evaluate consequences of radiation on electronics, these two specific capabilities allow addressing the issue of internal charging. The charging of thick dielectrics inside a spacecraft results from the deposit of penetrating charged particles in dielectrics having small conductivity. This charging can be mitigated by material conductivity, which is enhanced by dose deposition. Since Geant4 can supply three-dimensional maps of charge deposit and dose, it offers a very good opportunity to use these data to perform three-dimensional computations of internal charging. A specific version of SPIS called SPIS-IC (IC for Internal Charging) uses the Geant4 results as input in order to make an internal charging transport computation.

A first version of SPIS-IC has been presented at the SCTC in 2012 [8]. This version was already used to simulate the charge transport through conduction inside the dielectrics in a time dependent way. It permits to assess the internal ESD risk inside the S/C payload. As this software was a prototype, some improvements were needed to improve the integration accuracy and efficiency. The major concerns of this study are:

1) To improve the time dependents ability of the tool by improving the time scheme of transport solver and to model the time evolution of the conductivity

2) To improve the accuracy of the conduction model concerning the dependence on temperature, electric field, dose rate, charge and dose accumulated (i.e. time dependent aspect).

3) To validate the modelling chain by comparing the simulation results to experimental ones from simple

cases to more complex cases (i.e. on existing commercial component)

2.1. Simulation chain of internal charging

The internal charging solvers are based on the resolution of the following system of equation composed by the Poisson equation, the continuity equation for the net charge and the Ohm's law for the current calculation.

$$\begin{cases} \nabla \bullet (\varepsilon_0 \varepsilon_r \nabla V) = \rho \\ \dfrac{\partial \rho}{\partial t} + \nabla \bullet J = \dot{\rho} \\ J = \sigma E \end{cases} \tag{1}$$

This system of equations is solved in a 3D unstructured mesh that permits to have complex geometries. In this system of equations, the charge deposition (from Geant4) is directly visible as a source term of the continuity equation. The dose deposition is hidden in the current calculation in the conductivity term as it is explained later.

2.2. Time dependent resolution

In the standard SPIS-IC calculation, the system of equation (1) was solved with an explicit method. This implies for stability reason that the time step was limited regarding the transport time characteristic and the charge deposition characteristic times:

$$\Delta t < \min\left(\frac{\varepsilon_0 \varepsilon_r}{\sigma}, \frac{\rho}{\dot{\rho}} \right) \tag{2}$$

The time step is thus limited by the high conductivity elements and where the charge deposition is high. In order to avoid this limitation, we propose to (semi-)implicitly solve the Poisson equation by arranging the system of equation. We get a modified Poisson equation taking into account in a same equation the capacitive and the Ohmic effect of the charge deposition:

$$\nabla \bullet \left(\left(\varepsilon_0 \varepsilon_r + \sigma^{n-1} \Delta t \right) \nabla V^n \right) = \rho^{n-1} + \dot{\rho} \Delta t \tag{3}$$

In this new scheme, only the conductivity is treated explicitly. It means that the only time step limitation will be due to the time variation of the conductivity:

$$\Delta t < \frac{\sigma}{d\sigma / dt} \tag{4}$$

2.3. Conductivity model enhancement

Conventional codes used for space charging assessment (SPIS [9], ELSHIELD [8], NASCAP [10],…) use very simple law in which RIC depends only on radiation dose rate:

$$RIC = K.\left(\frac{dD}{dt} \right)^{\Delta} \tag{5}$$

where K and Δ are empirical parameters derived from dedicated experiments.

This relation, developed by Rose [11], corresponds to steady state RIC for which equilibrium is reached between generation, trapping and recombination. In reality, the equilibrium state can be reached after a long time (weeks or months), due for example to low recombination rates. It is also well known that, in reality for low electron flux such as in space, the RIC depends on radiation dose, radiation dose rate, material conditions (temperature, impinging electron energy, light), charging state (electric field), and its microscopic state and structure (trap energy distribution, polarisability,…). It has been especially demonstrated in [12]–[14] that the RIC of most polymers evolves steeply with radiation time (due to the steady change of free charge density with the increasing radiation dose).

Dependence of RIC with radiation dose has been described using a simple model in analogy with a solid state band models describing evolution of free and trapped charges (electrons n and holes p) as a function of time, carrier generation rate g, trapping τ, de-trapping τ_t and recombination α parameters, as described below:

$$\begin{aligned} \frac{dn}{dt} &= g - \alpha n p_t - \frac{n}{\tau_n} + \frac{n_t}{\tau_{nt}} \\ \frac{dn_t}{dt} &= \frac{n}{\tau_n} - \frac{n_t}{\tau_{nt}} - \alpha p n_t \\ \frac{dp}{dt} &= g - \alpha n_t p - \frac{p}{\tau_p} + \frac{p_t}{\tau_{pt}} \\ \frac{dp_t}{dt} &= \frac{p}{\tau_p} - \frac{p_t}{\tau_{pt}} - \alpha n p_t \end{aligned} \tag{6}$$

In this model the net current is coming from the mobility of the free charges (μ_e et μ_p the mobility of electrons and holes):

$$J = e\left(p.\mu_p - n.\mu_e \right) E = \sigma E \tag{7}$$

This model [13] is solved in SPIS for each mesh of the discretized computational volume. It could be noted that, in the system (6), the transport of electron and holes is neglected. The effect of this assumption is discussed in [15].

3. EXPERIMENTAL SETUP

In the frame of the validation of the model, two irradiation facilities available at ONERA/DESP have been used.

3.1. SINERE facility

SIRENE is a sophisticated and unique test facility especially designed for the study of surface and internal charging of space materials and satellite components under extreme environment (usually geostationary orbit radiation conditions). This facility is able to reproduce the geostationary electron spectrum (in the energy range [0-400 keV]). It allows realistic assessment of voltage built up in geostationary orbit. Its flexibility allows the simulation of extreme environments different than the geostationary one (eg, MEO, LEO or other planetary radiation environments). This facility is widely used as well for the characterization of radiation induced conductivities of space materials. It is instrumented with a contact-less electrostatic probe, current measurement systems and non-contact PEA device. The temperature of the sample holder can be controlled in the range [-180 °C, +250 °C] allowing to reproduce the temperature variations of materials on flight. A pumping system allows experiments at vacuum of around 10^{-6} hPa. Thanks to these different experimental specifications and its spectrum flexibility, the SIRENE experimental facility is highly relevant for the current study for the energy range [7-400 keV]. Both electron sources shall allow then adjusting electron energy between 7 and 400 keV. Large electron flux range can be achieved, between 0.1 pA.cm^{-2} to 5 nA.cm^{-2} that is representative of the incoming fluxes met for internal charging issue.

3.2. GEODUR facility

GEODUR is a radiation test facility allowing the study of satellite internal and surface charging, evaluation of RIC of thick materials and sample radiative ageing using 400 keV to 2.5 MeV monoenergetic electrons. It is equipped with a 2.5 MeV Van de Graaff electron accelerator and a double scattering system for the production of a distributed electron spectrum in the energy range [200 keV – 1 MeV]. It is instrumented with a contact-less electrostatic probe and current measurement systems for the characterisation of internal charging behaviour of space elements. The temperature of the sample holder can be controlled in the range [-180 °C, +250 °C] allowing to reproduce the temperature variations of materials on flight. A pumping system allows experiments at vacuum of around 10^{-6} hPa. This facility has been used for this study especially for irradiation at energies higher than 400 keV, low electron flux (this parameter can be adjusted between 0.1 pA.cm-2 to 10 nA.cm^{-2}), long irradiation time.

4. VALIDATION PROTOCOL

The proposed test plan is divided into four main test batches which mainly differ by the sample geometry and the characterisation procedure. The overall objective of this test plan is to be able to validate the implemented physical model and algorithm through a large batch of sample geometry and grounding configuration for which the sample surface is or not kept free of grounded and floating tracks. Two main characterization techniques have been used in these experimental tests : Kelvin probe for the measurement of surface potential, and non-contact PEA for the measurement of bulk charge density.
The four batches have been chosen with an increasing complexity. Batch 1 is a simple thin sample of one dielectric or a geometric step considering a change of thickness at one position. Batch 2 represents a simple electric circuit or a motherboard, i.e. an epoxy sample with metallic patches. Batch 3 is a D-type connector. Batch 4 is an optical lens.

5. RESULTS AND DISCUSSION

The results of all the four batches are not discussed in detail. In this paper, we focus on two tests which correspond to the step geometry of batch 1 and the batch 3. The batches 2 and 4 do not show any RIC effect on charging and are less interesting. The simple planar case of batch 1 is detailed in another paper [15].

5.1. Dielectric step case

The first geometry tested is represented in Fig. 1. It has been tested under a 350 keV electron irradiation. As we can see, it is a step geometry (two slabs configuration) with two different thicknesses, 1 mm and 0.5 mm.

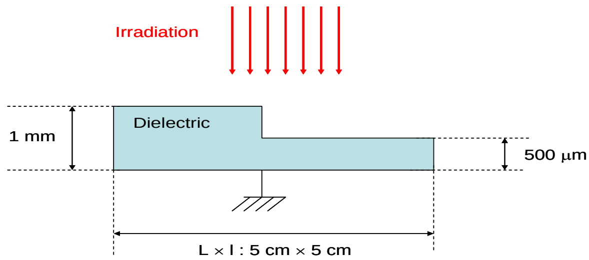

Figure 1: Schematic representation of the step geometry.

As it can be seen on the top of Fig. 2, the energy deposited computed by Geant 4 shows that the electron flux does not go through the left hand side and completely irradiate the right hand side parts. It makes this configuration a 3D issue.

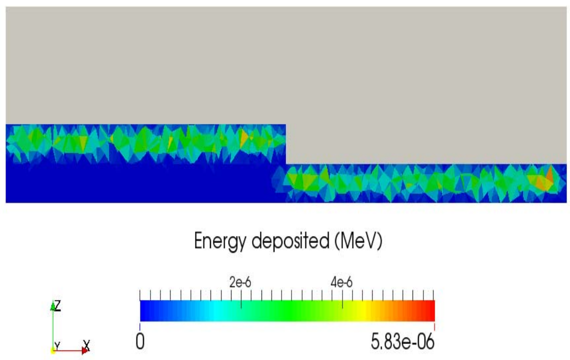

Figure 2: Dose deposited in MeV by incident e- at 0.35 MeV (calculation from Geant4/GRAS).

Fig. 3 represents the time evolution of the potential on the two steps of the geometry. The highest potential is on the thickest zone an the smaller potential on the thinnest zone. We can observe that in the smaller step the irradiation completely irradiate the volume thus the conductivity is high everywhere. It results that the potential are small during the irradiation. On the thickest zone, all the electrons are stopped at about the middle of the thickness. Thus this zone charges until a conductive path permits a charge flow toward the smaller step. This conductive path is brought into evidence by the high relaxation kinetics observed on the larger step.

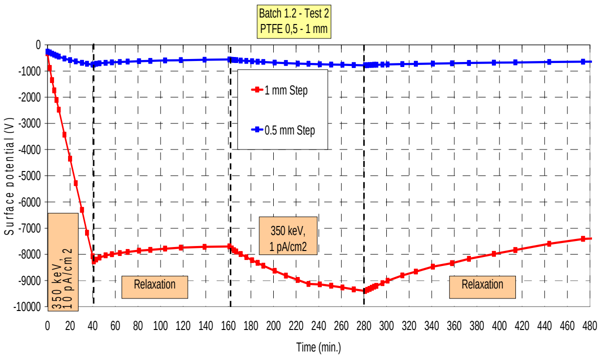

Figure 3: Measurement of surface potential evolution with irradiation at 350 keV on PTFE step sample

The measurements are globally in good agreement with the simulations performed and presented on Fig. 4. The only discrepancy comes from a higher relaxation during the relaxation phase due to an overestimation of the delayed RIC.

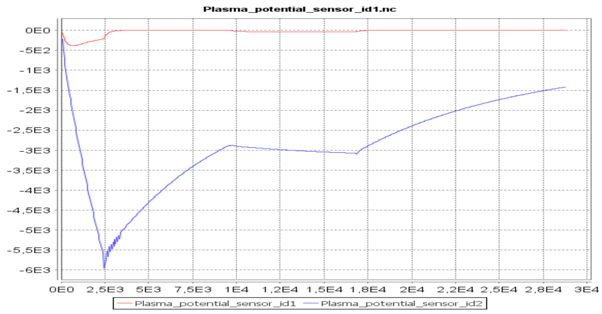

Figure 4: Simulation results of surface potential evolution with irradiation at 350 keV on PTFE step sample

Fig. 5 represents the conductivity inside the dielectric at the end of the first irradiation phase. We can clearly observe the conductive path between both zones.

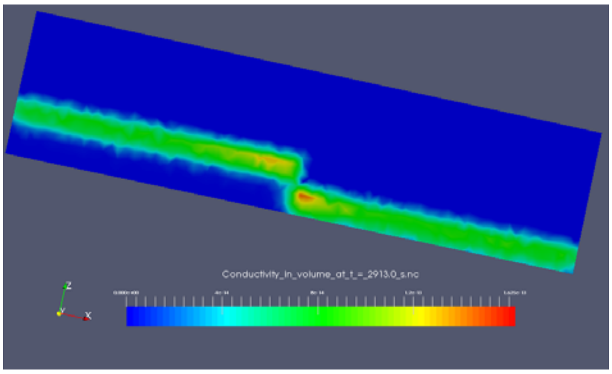

Figure 5: Cconductivity map in the dielectric at t = 2900s and energy of 350keV

5.2. D-Type connector case

The following results present the evolution of surface potential measured on the 25 pins d-type connector (represented on Fig. 6) irradiated with monoenergetic electrons at 400 keV and 1.9 pA.cm^{-2}.

a) 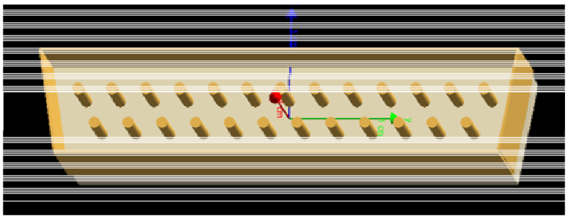

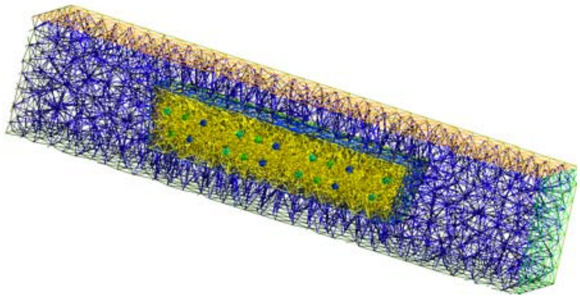
b)

Figure 6: a) geometrical model and b) mesh of the 25 pins D-Type connector.

Fig. 7 represents the evolution of the potential of two metallic flags connected to two groups of three pins inside the dielectric and a measurement of the surface potential on top of the connector dielectric. On this figure, during the first irradiation / relaxation phase, we can see a high charging kinetics on the insulating part and on both flags with similar surface potentials on these different parts.

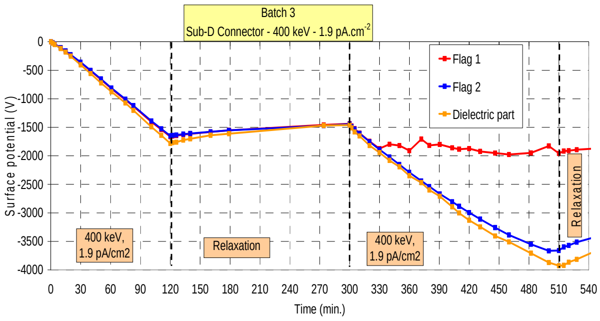

Figure 7: Evolution of surface potential during the test performed on 25 pins d-type connector

We can however notice during the second irradiation phase that the surface potential on Flag 1 deviates from the other ones, while relaxation kinetics (last phase) is lower. A conductive path has been created, certainly between the pins connected to flag 1 and one grounded pins, when reaching a given surface potential. This would be equivalent to a Zener effect. The surface potential is then frozen at a given potential during irradiation and relaxation. Below this level, the material gets highly resistive and potential can not then decrease during relaxation. Above this level, charge leakage is high allowing a stabilization of potential during irradiation.

The simulations are in good agreement with the experiments. The simulations results permit to analyse the situation and to see that the electric field is very high around the group of pins of Flag 1. This could explain the occurrence of a Zener like effect.

6. CONCLUSIONS

This paper presents an advanced model of radiation and charging able to model time dependent and three dimensional effects. In particular, the conductivity model implemented on this new version of SPIS-IC goes well upon the state on the art for 3D charging models. The results are in good agreement with the experiments. Some discrepancies are nevertheless visible between the model and the experiments. This requires a further analysis of the experimental results and the conductivity model.

7. ACKNOWLEDGEMENTS

This work has been performed in the frame of the ESA/ESTEC contract 4000110897/14/NL/AK. The authors want also thanks the CNES for his support through the CNES/R&T program.

8. REFERENCES

[1] H. B. Garrett, I. Katz, I. Jun, W. Kim, A. C. Whittlesey, and R. C. Evans, "THE JOVIAN CHARGING ENVIRONMENT AND ITS EFFECTS—A REVIEW," in *Proceedings of 11th Spacecraft Charging Technology Conference*, Albuquerque, NM, 2010.

[2] I. Katz, "A 3-D Model of Circuit Board Internal Electrostatic Charging," in *Proceedings of 11th Spacecraft Charging Technology Conference*, Kitakyushu, Japan, 2010.

[3] C. L. Lemon, J. L. Roeder, M. D. Looper, J. F. Fennell, M. J. Meshishnek, and M. R. Ciafalo, "A 3-D Model of the Internal Charging of Spacecraft Dielectric Materials," in *Proceedings of 11th Spacecraft Charging Technology Conference*, Kitakyushu, Japan, 2010.

[4] A. Whittlesey, "Avoiding problems caused by spacecraft on-orbit internal charging effects," *NASA Wash. DC NASA-HDBK-4002*, 1999.

[5] J. Allison, K. Amako, J. Apostolakis, H. Araujo, P. Arce Dubois, M. Asai, G. Barrand, R. Capra, S. Chauvie, R. Chytracek, G. A. P. Cirrone, G. Cooperman, G. Cosmo, G. Cuttone, G. G. Daquino, M. Donszelmann, M. Dressel, G. Folger, F. Foppiano, J. Generowicz, V. Grichine, S. Guatelli, P. Gumplinger, A. Heikkinen, I. Hrivnacova, A. Howard, S. Incerti, V. Ivanchenko, T. Johnson, F. Jones, T. Koi, R. Kokoulin, M. Kossov, H. Kurashige, V. Lara, S. Larsson, F. Lei, O. Link, F. Longo, M. Maire, A. Mantero, B. Mascialino, I. McLaren, P. Mendez Lorenzo, K. Minamimoto, K. Murakami, P. Nieminen, L. Pandola, S. Parlati, L. Peralta, J. Perl, A. Pfeiffer, M. G. Pia, A. Ribon, P. Rodrigues, G. Russo, S. Sadilov, G. Santin, T. Sasaki, D. Smith, N. Starkov, S. Tanaka, E. Tcherniaev, B. Tome, A. Trindade, P. Truscott, L. Urban, M. Verderi, A. Walkden, J. P. Wellisch, D. C. Williams, D. Wright, and H. Yoshida, "Geant4 developments and applications," *IEEE Trans. Nucl. Sci.*, vol. 53, no. 1, pp. 270–278, Feb. 2006.

[6] J. Allison, J. Cueto, V. Grichine, A. Howard, S. Ibarnia, V. Ivanchenko, M. Maire, G. Santin, and L. Urban, "New Geant4 Model and Interface Developments for Improved Space Electron Transport Simulations: First results," in *RADECS 2011 Proceedings*, 2011.

[7] "Spis website: http://dev.spis.org/."

[8] P. Sarrailh, D. Sarrail, J.-C. Mateo-Velez, J. F. Roussel, J. Forest, D. Rodgers, G. Santin, and J. Cueto, "Three-Dimensional Model of Internal Charging using SPIS," in *Proceedings of 12th Spacecraft Charging Technology Conference*, Kitakyushu, Japan, 2012.

[9] J. Roussel, F. Rogier, G. Dufour, J.-C. Mateo-Velez, J. Forest, A. Hilgers, D. Rodgers, L. Girard, and D. Payan, "SPIS open-source code: Methods, capabilities, achievements, and prospects," *Plasma Sci. IEEE Trans. On*, vol. 36, no. 5, pp. 2360–2368, 2008.

[10] V. A. Davis, M. J. Mandell, D. C. Cooke, A. Wheelock, J.-C. Mateo-Velez, J.-F. Roussel, D. Payan, M. Cho, and K. Koga, "Comparison of Low Earth Orbit Wake Current Collection Simulations Using Nascap-2k, SPIS, and MUSCAT Computer Codes," *IEEE Trans. Plasma Sci.*, vol. 41, no. 12, pp. 3303–3309, décembre 2013.

[11] A. Rose, "Recombination Processes in Insulators and Semiconductors," *Phys. Rev.*, vol. 97, no. 2, pp. 322–333, Jan. 1955.

[12] T. Paulmier, B. Dirassen, D. Payan, and M. Van Eesbeek, "Material charging in space environment: Experimental test simulation and induced conductive mechanisms," *Dielectr. Electr. Insul. IEEE Trans. On*, vol. 16, no. 3, pp. 682–688, 2009.

[13] R. Hanna, T. Paulmier, P. Molinie, M. Belhaj, B. Dirassen, D. Payan, and N. Balcon, "Radiation Induced Conductivity in Teflon FEP Irradiated With Multienergetic Electron Beam," *IEEE Trans. Plasma Sci.*, vol. 41, no. 12, pp. 3520–3525, Dec. 2013.

[14] T. Paulmier, B. Dirassen, M. Arnaout, D. Payan, and N. Balcon, "Radiation induced conductivity of space used polymers under high energy electron irradiation," presented at the 13th Spacecraft Charging Conference, Pasadena, CA, USA, 2014.

[15] R. Pacaud, T. Paulmier, and P. Sarrailh, "1D Physical Model of Charge Distribution and Transport in Dielectric Materials Under Space Radiations," *14th Spacecraft Charging Technology Conference*, Noordwijk, NL, 04-Apr-2016.